

DOI:10.1002/ejic.201402420

Aminoalkyl-1,1-bis(phosphinic acids): Stability, Acid–Base, and Coordination Properties

Tomáš David,^[a] Soňa Procházková,^[a] Jan Kotek,^[a]
Vojtěch Kubiček,^{*[a]} Petr Hermann,^[a] and Ivan Lukeš^[a]

Keywords: Ligand design / O ligands / Phosphinic acids / Hydrolytic stability / Stability constants / Acidity

Four geminal bis(phosphinic acids), namely, aminomethyl-bis(*H*-phosphinic acid) (H_2L^1) and 4-aminobutyl-1-hydroxy-1,1-bis(*R*-phosphinic acid) with $R = H$ (H_2L^2), Me (H_2L^3) and CH_2CH_2COOH (H_4L^4), were studied. Their acid–base properties and coordination ability towards Cu^{2+} , Ni^{2+} and Zn^{2+} ions were studied by potentiometry, UV/Vis spectroscopy and NMR spectroscopy. The amine group in H_2L^1 has a lower protonation constant ($\log K_a = 6.79$) than those found for other studied bisphosphinates ($\log K_a = 10.75$ – 11.05) with distant amine groups. The structure of $[Ca(H_2L^2-$

$O,O')](HL^2-O,O')]Cl$ revealed an octahedral arrangement of the metal coordination sphere and a linear polymeric structure, which forms through eight-membered $Ca(-O-P-O-)_2Ca$ rings. The structure of $[Cu(HL^3-O,O')_2(H_2O)] \cdot 5H_2O$ shows two chelating bisphosphinate groups in an equatorial O_4 environment. The structure of $[Cu(H_{0.5}L^3-O,O')(NO_3)_{0.5}] \cdot 2.25H_2O$ shows two different coordination environments, one is an elongated tetragonal pyramid, and the other is a trigonal bipyramid with a bidentate nitrate ion.

Introduction

Geminal bisphosphonates (BPs) are an important group of organophosphorus compounds. The proximity of two phosphonate groups leads to strong chelating ability^[1] and strong interactions with the surfaces of various inorganic materials.^[2,3] Their high affinity to hydroxyapatite, which is the main inorganic component of bone tissue, provides extensive medical applications in the treatment of osteoporosis and other diseases of calcified tissues.^[4] The anchoring of BPs on the surface of titanium dioxide,^[5–7] iron oxides^[8–11] and many other inorganic materials has been employed in a broad range of academic and industrial applications.^[2,3,12,13] An important class of BPs are those that bear an amine group in the side chain. They show specific pharmaceutical properties and, in addition, the amine group can be utilized as a reactive moiety for the attachment of various functionalities such as different drugs, fluorescent labels, complexes of metal radioisotopes or peptides to deliver their cargo to bone or calcified tissues.^[12–15] Bisphosphonates may also act as inhibitors in biochemical pathways as they interact with the metal ions that are typically present in the active centres of enzymes such as adenosinetriphosphatases (ATPases), farnesyl transferase, squalene synthase

or tyrosine phosphatase,^[16] however, their high hydroxyapatite affinity excludes any biomedical application that is not related to bone tissue.

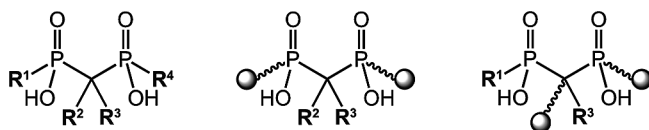
The coordination properties of the geminal bisphosphonate group have been found to be very advantageous. Thus, polydentate ligands bearing this group have been designed and synthesized, and their coordination to metal ions in aqueous solutions as well as in the solid state has been investigated.^[1] The geminal bisphosphonate group interacts strongly with hard metal ions and often bridges two or more metal ions to form polymeric structures. Owing to its excellent coordination ability, the bisphosphonate group might be considered as an excellent building block in the design of polydentate ligands. These ligands are mainly investigated as metal carriers for biomedical applications such as magnetic resonance imaging (MRI), radiodiagnosis [positron emission tomography (PET) and single-photon emission computed tomography (SPECT)] or radiotherapy. However, the strong adsorption to bone mineral and the strong affinity to inorganic materials disable some applications of the bisphosphonate conjugates in biomedical fields.

This disadvantage of bisphosphonates could be overcome through the use of geminal bisphosphinates (Scheme 1), which have a similar metal-ion binding motif to that of BPs but show negligible adsorption on inorganic surfaces.^[17,18] Unlike BPs, much less attention has been devoted to geminal bisphosphinates,^[19–21] and only a few complexation studies have been published.^[22] Whereas research on BPs is mostly focused on bone or calcium-related issues, bisphosphinates might be studied as inhibitors of

[a] Department of Inorganic Chemistry, Faculty of Science, Charles University in Prague, Hlavova 2030, 128 40 Prague 2, Czech Republic
E-mail: kubiček@natur.cuni.cz
www: <http://web.natur.cuni.cz/anorchem/19/>

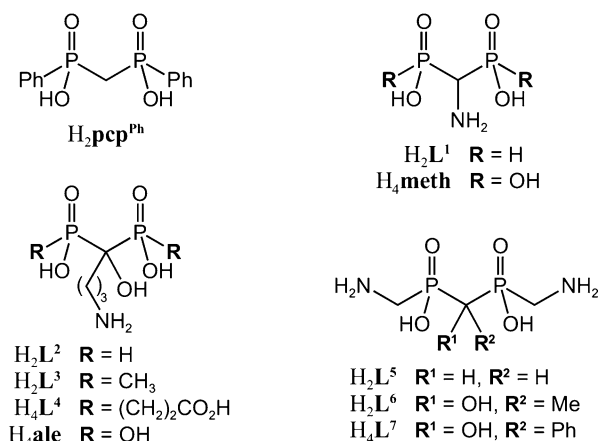
Supporting information for this article is available on the WWW under <http://dx.doi.org/10.1002/ejic.201402420>.

various enzymes or as chelating groups in biomedical applications for which strong bone affinity is undesirable. Furthermore, bisphosphinates offer new structural motifs (Scheme 1) as each phosphinate group can be attached to two carbon atoms. This allows the synthesis of polydentate ligands bearing bisphosphinate groups in the middle of a polyamine chain, for example, and fine tuning of the coordination properties of such ligands. Owing to their chain-forming ability, the bisphosphinate ligands might be interesting building blocks for metal–organic framework (MOF) materials.



Scheme 1. General structure of bisphosphinates and their possible utilization as chain-forming groups.

Recently, we have reported on 1-hydroxyalkyl-bis(*H*-phosphinic acids)^[18] and symmetrical methylene-bis-[(aminomethyl)phosphinic acids] (Scheme 2, H₂L⁵–H₂L⁷) with amine groups at the opposite ends of the molecules.^[23] As a continuation of this study, we present here four geminal bisphosphinates, H₂L¹, H₂L², H₂L³ and H₄L⁴, with an aminoalkyl group attached to the central carbon atom (Scheme 2). They are analogues of aminomethyl-bis(phosphonic acid) (H₄meth) and 4-aminobutyl-1,1-bis(phosphonic acid) (alendronate, H₄ale). The acid–base properties and coordination ability of these new bisphosphinates were studied to get more information on this class of chelating agents and to define structural motifs suitable for molecules/conjugates for which low bone affinity and a rather weak complexing power are necessary requirements. The data will be used in the design of polydentate ligands for biomedical applications.

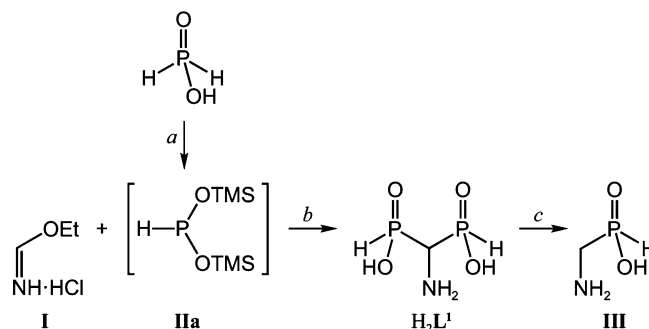


Scheme 2. Structures of studied aminoalkyl-1,1-bisphosphinates and related compounds.

Results and Discussion

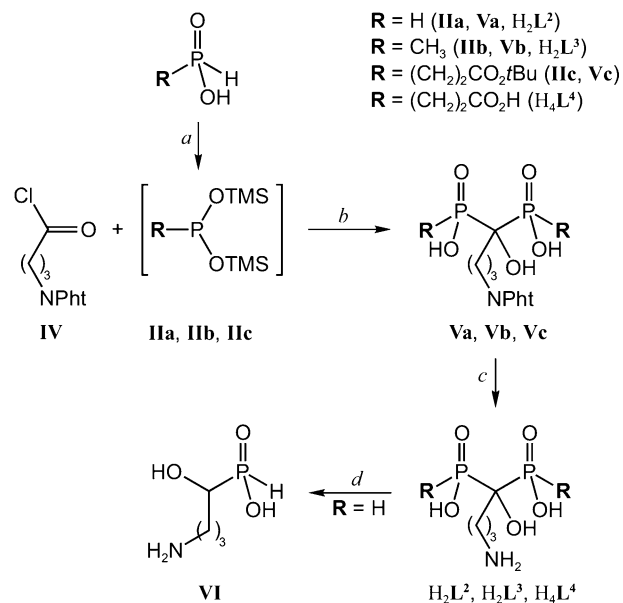
Synthesis and Stability of the Ligands

The synthetic pathways used for preparation of H₂L¹, H₂L², H₂L³ and H₄L⁴ are depicted in Schemes 3 and 4. Compound H₂L¹ was synthesized by modification of the previously reported method that utilizes the reaction of ethyl formimidate (**I**) with bis(trimethylsilyl)hypophosphite (**IIa**).^[24] Our approach employs the in situ formation of the pyrophoric phosphine **IIa** and an easy purification without the need to distil the silylated intermediate. Compounds H₂L², H₂L³ and H₄L⁴ were synthesized by the reaction of the *N*-protected 4-aminobutanoyl chloride **IV** with 2 equiv. of phosphine **IIa** or the appropriate bis(trimethylsilyl)phosphonite **IIb** or **IIc**. The reaction is analogous to those previously reported for geminal bis(*H*-phosphinates)^[18,25] and for cyclic aminobisphosphinates.^[20] The protected intermediates **Va–Vc** were treated with aqueous HCl or with hydrazine to remove the phthalimide protecting group; the *tert*-butyl ester groups of **Vc** were also removed during the reaction with hydrazine. The reaction mixture obtained after the deprotection of **Vc** contained a side-product (ca. 30%), which was identified as the monohydrazide of H₄L⁴ (Figure S1).



Scheme 3. Synthesis of H₂L¹. Reagents and conditions: (a) HMDS, 100 °C; (b) 1. CH₂Cl₂, r.t.; 2. EtOH, r.t.; (c) 1 M aq. HCl, 80 °C.

The bis(phosphinic acids) H₂L¹ and H₂L² show limited stability in aqueous solutions owing to the presence of geminal *H*-phosphinic acid groups. The decomposition is very slow in alkaline solutions (1 M aq. NaOH), and only traces (<10%) of decomposition products were found after 20 d at 80 °C. On the contrary, both compounds show complete decomposition in acidic media (1 M aq. HCl). The half-lives of H₂L¹ and H₂L² were 3.2 and 194 h at 80 °C, respectively (Figure S2). In the latter case, the value is in the same range as the half-lives previously reported for other geminal bis(*H*-phosphinic acids)^[18] and the decomposition (formally, hydrolysis) yields the appropriate α -hydroxyalkyl(*H*-phosphinic acid) **VI** and phosphorous acid. On the contrary, the decomposition of H₂L¹ in acidic solution is significantly faster, which indicates the low stability of the aminomethyl-bis(*H*-phosphinic acid) fragment. The decomposition quantitatively yields aminomethyl-(*H*-phosphinic acid) (**III**, Scheme 3)^[26] and 4-amino-1-hydroxybutylphosphinic acid (**VI**, Scheme 4);^[27] it could be considered as a new syn-



Scheme 4. Synthesis of the studied bisphosphinates. Reagents and conditions: (a) TMSCl/DIPEA, CH₂Cl₂, r.t.; (b) 1. CH₂Cl₂, r.t.; 2. EtOH, r.t.; (c) N₂H₄·H₂O in EtOH, r.t.; or conc. aq. HCl, reflux; (d) 1 M aq. HCl, 80 °C. Pht = phthaloyl.

thetic route for the preparation of *H*-phosphinic acids. On the other hand, H₂L³ and H₄L⁴ are fully stable in aqueous solution at any pH.

Acid–Base and Coordination Properties

The solution behaviour of the hydrolytically stable geminal bisphosphinates H₂L³ and H₄L⁴ and their complexes was studied by potentiometry. In parallel, the protonation constant of the amine group, which is the crucial factor for the coordination properties of the ligands, was determined by NMR titration of H₂L¹ and H₂L² (Figures S3 and S4). The values of the protonation constants are summarized in Table 1. The highest constant was assigned to the protonation of the amine group (for the protonation schemes see Schemes S1 and S2). The basicity of the amine group in H₂L¹ was found to be significantly lower than those of H₂L², H₂L³ and H₂L⁴ owing to the presence of two proximate strongly electron-withdrawing *H*-phosphinate groups. In addition, the basicities of the studied compounds are significantly lower than those published for the analogous BPs H₄meth and H₄ale (Scheme 2, Table 1).^[28] This could be explained by the lower charge of the deprotonated phos-

phinate groups in comparison with that of fully ionized phosphonates; the fully deprotonated phosphonate group is strongly electron-donating and increases the basicity of adjacent amine groups.^[29] The other protonation constants of H₂L³ are ascribed to the protonation of the bisphosphinate groups and they are similar to those previously published for H₂pcp^{Ph} (Scheme 2, Table 1).^[30] For H₄L⁴, the next two protonations are for the carboxylate groups, and the last determined protonation constant belongs to a phosphinate group. The values are in the expected range for the –PO₂[–]–CH₂CH₂CO₂[–] fragment.^[31,32] The protonation constant of the second phosphinate group was not accessible as it is too low to be determined by potentiometry. The hydroxy group cannot undergo deprotonation in aqueous solution unless metal ions are present (see below).

The coordination properties of the bisphosphinates were studied in the systems with Cu²⁺, Zn²⁺ and Ni²⁺ ions for 1:1, 1:2 and 2:1 (2:1 only for ligand H₄L⁴) metal/ligand ratios. The results are summarized in Tables 2 and S1, and the distribution diagrams are shown in Figures 1 and S5–S10. The dominant complexes formed are those with 1:1 M/L ratios. Complexation starts at pH < 2 with the formation of protonated complexes. The protons are very probably localized on the amine and/or carboxylate groups (for H₄L⁴). The stability constants (log *K*_{ML}) are higher for H₄L⁴, in agreement with the higher basicity of its amine group and with the higher denticity of the ligand owing to presence of the additional carboxylate group. The lower overall basicities of H₂L³ and H₄L⁴ lead to lower stability constants for their complexes than the log *K*_{ML} values for the complexes of their bisphosphonate analogues H₄meth and H₄ale (Table 2).^[28] Surprisingly, the Zn²⁺ complexes show higher stability than the Ni²⁺ complexes, which points to a rather hard character for the studied bisphosphinate ligands.

The protonation constants of the [LM] or [HLM] species indicate that the protons are bound to distant amine and/or carboxylate groups, and the ligands are probably coordinated only through the phosphinate groups, as was similarly found for the complexes in the solid state (see below). In most of the studied systems, the stabilities of the complexes are not high enough to prevent the precipitation of the metal hydroxides and, thus, the titrations had to be terminated in the neutral region. That was not the case for the Cu²⁺/H₂L³, Cu²⁺/H₄L⁴ and Ni²⁺/H₂L³ systems, for which [H_{–1}LM] and [H_{–2}LM] species were identified; here, the negative index values represent the formation of hydroxido

Table 1. Overall (log β) and stepwise (p*K*_a) protonation constants of the studied geminal bisphosphinates and related ligands.

Species	H ₂ L ¹ [a]	H ₂ L ² [a]	H ₂ L ³ [b]		H ₄ L ⁴ [b]		H ₄ meth[c]	H ₄ ale[c]	H ₂ pcp ^{Ph} [d]
	p <i>K</i> _a	p <i>K</i> _a	log β	p <i>K</i> _a	log β	p <i>K</i> _a	p <i>K</i> _a	p <i>K</i> _a	p <i>K</i> _a
HL	6.79(2)	10.78(3)	10.75(1)	10.75	11.05(1)	11.05	11.43	12.68	3.33
H ₂ L	[e]	[e]	14.38(2)	3.63	16.43(1)	5.38	8.29	11.07	1.35
H ₃ L	[e]	[e]	16.33(2)	1.95	20.74(1)	4.31	5.35	6.36	–
H ₄ L	–	–	–	–	23.35(1)	2.61	1.18	2.19	–

[a] This work, determined by ¹H and ³¹P NMR spectroscopy (25 °C, without ionic strength control). [b] This work, determined by potentiometry (25 °C, *I* = 0.1 M KNO₃). [c] Determined by potentiometry [25 °C, *I* = 0.1 M (NMe₄)Cl].^[28] [d] Determined by potentiometry [25 °C, *I* = 0.5 M (NMe₄)Cl].^[30] [e] Not determined owing to the low stability of the compounds under acidic conditions.

Table 2. Equilibrium constants (25 °C, $I = 0.1 \text{ M KNO}_3$) of the complexes in the systems containing the title ligands and selected divalent metal ions. The negative hydrogen stoichiometry represents the formation/coordination of alcoholate anion or formation of hydroxido complexes.

Metal ion	Equilibrium	H_2L^3	H_4L^4
Cu^{2+}	$\text{Cu}^{2+} + (\text{L})^{2-} \rightleftharpoons [\text{Cu}(\text{L})]$	8.12	9.25
	$\text{Cu}^{2+} + (\text{HL})^- \rightleftharpoons [\text{Cu}(\text{HL})]^+$	4.58	5.67
	$[\text{Cu}(\text{L})] + \text{H}^+ \rightleftharpoons [\text{Cu}(\text{HL})]^+$	7.21	7.47
	$[\text{Cu}(\text{HL})]^+ + \text{H}^+ \rightleftharpoons [\text{Cu}(\text{H}_2\text{L})]^{2+}$	–	4.68
	$[\text{CuH}_{-1}(\text{L})]^- + \text{H}^+ \rightleftharpoons [\text{Cu}(\text{L})]$	6.69	7.67
	$[\text{CuH}_{-2}(\text{L})]^{2-} + \text{H}^+ \rightleftharpoons [\text{CuH}_{-1}(\text{L})]^-$	11.97	11.50
	$[\text{Cu}(\text{HL})]^+ + (\text{HL})^- \rightleftharpoons [\text{Cu}(\text{HL})_2]$	2.66	–
	$[\text{Cu}(\text{L})]^{2-} + \text{Cu}^{2+} \rightleftharpoons [\text{Cu}_2(\text{L})]$	–	4.67
Zn^{2+}	$\text{Zn}^{2+} + (\text{HL})^- \rightleftharpoons [\text{Zn}(\text{HL})]^+$	4.00	4.01
	$[\text{Zn}(\text{HL})]^+ + \text{H}^+ \rightleftharpoons [\text{Zn}(\text{H}_2\text{L})]^{2+}$	2.77	4.65
	$[\text{Zn}(\text{HL})]^+ + (\text{HL})^- \rightleftharpoons [\text{Zn}(\text{HL})_2]$	2.74	–
	$[\text{Ni}(\text{HL})]^{2+} + \text{H}^+ \rightleftharpoons [\text{Ni}(\text{H}_2\text{L})]^{3+}$	3.05	3.36
Ni^{2+}	$[\text{NiH}_{-1}(\text{L})]^- + 2\text{H}^+ \rightleftharpoons [\text{Ni}(\text{HL})]^+$	2×8.53	–
	$[\text{NiH}_{-2}(\text{L})]^{2-} + \text{H}^+ \rightleftharpoons [\text{NiH}_{-1}(\text{L})]^-$	10.65	–

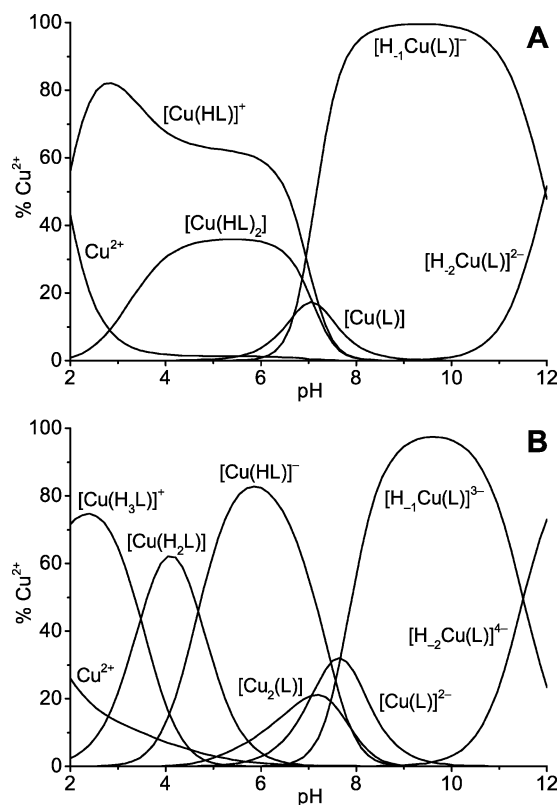


Figure 1. Distribution diagrams of (A) $\text{Cu}^{2+}\text{-H}_2\text{L}^3$ ($c_{\text{L}} = 4 \text{ mM}$, $c_{\text{Cu}} = 2 \text{ mM}$) and (B) $\text{Cu}^{2+}\text{-H}_4\text{L}^4$ ($c_{\text{L}} = c_{\text{Cu}} = 4 \text{ mM}$) systems.

complexes or metal-induced deprotonation of the hydroxy group attached to the bridging carbon atom. For both H_2L^3 and H_4L^4 , the high abundance and broad dominance range of the $[\text{H}_{-1}\text{ML}]$ species as well as their electronic spectra (see below) point to deprotonation of the central hydroxy group. The close proximity of two strongly electron-withdrawing phosphinate groups increases the acidity of the hydroxy group and, thus, the metal ions induce its deprotonation and simultaneous coordination even at neutral

pH. In addition, the metal-induced deprotonation is driven by the formation of two five-membered chelate rings. Analogous behaviour has been reported recently for the *P*-methylhydroxy group of the hydroxymethylene-bis[(amino-methyl)phosphinates] H_2L^5 and H_2L^6 (Scheme 2)^[22] and macrocyclic complexes bearing *N*-methylene(hydroxymethyl)phosphinate pendant arms.^[32,33]

For both H_2L^3 and H_4L^4 , species with different stoichiometries were also identified. The high denticity of H_4L^4 allows the formation of dinuclear $[\text{LM}_2]$ complexes. On the contrary, owing to its lower denticity, H_2L^3 forms $[\text{H}_2\text{L}_2\text{M}]$ species, in which the coordination of two ligand molecules protonated on the distant amine group is supposed (see below). The coordination of the second ligand molecule or the second metal ion is not thermodynamically favoured and, thus, both types of complexes are present in solution as minor species (Figure 1).

To obtain more information about the coordination modes in the species suggested by the potentiometric models, the UV/Vis spectra of the $\text{Cu}^{2+}\text{-H}_2\text{L}^3$ and $\text{Cu}^{2+}\text{-H}_4\text{L}^4$ systems were recorded under conditions under which one species is dominant in solution according to the distribution diagrams (Figures 1, S5 and S8). At slightly acidic pH, light blue protonated species are present in solution. Their electronic spectra (Figure 2) show d-d transitions with maxima at 792 ($\epsilon = 30 \text{ M}^{-1}\text{cm}^{-1}$) and 776 nm ($\epsilon = 35 \text{ M}^{-1}\text{cm}^{-1}$) and ligand-to-metal charge transfer (CT) bands with maxima at 212 ($\epsilon = 2500 \text{ M}^{-1}\text{cm}^{-1}$) and 218 nm ($\epsilon = 3030 \text{ M}^{-1}\text{cm}^{-1}$) for

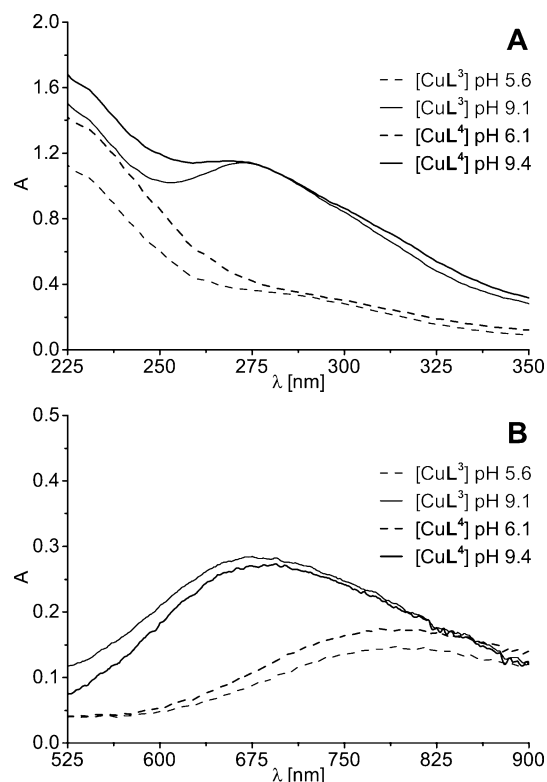


Figure 2. UV/Vis spectra of Cu^{2+} complexes with H_2L^3 and H_4L^4 (25 °C, water). (A) $c_{\text{M}} = 0.5 \text{ mM}$, $c_{\text{L}} = 1.0 \text{ mM}$; (B) $c_{\text{M}} = 5 \text{ mM}$, $c_{\text{L}} = 10 \text{ mM}$.

the complexes of H_2L^3 and H_4L^4 , respectively. The spectra are similar to those of $[\text{Cu}(\text{H}_2\text{O})_6]^{2+}$, which suggests that they have a coordination sphere formed by the oxygen atoms of the phosphinate groups and water molecules as observed in the solid state (see below). At slightly alkaline pH, at which the $[\text{H}_1\text{LCu}]$ species are exclusively present, the solution changed to a more intensive green in accordance with the shift of the d–d transition maxima {673 nm, $\epsilon = 57 \text{ M}^{-1} \text{ cm}^{-1}$ for $[\text{Cu}(\text{H}_1\text{L}^3)]^-$ and 694 nm, $\epsilon = 55 \text{ M}^{-1} \text{ cm}^{-1}$ for $[\text{Cu}(\text{H}_1\text{L}^4)]^{3-}$. In addition to the high-energy CT bands, additional UV bands with maxima at 272 ($\epsilon = 2280 \text{ M}^{-1} \text{ cm}^{-1}$) and 268 nm ($\epsilon = 2300 \text{ M}^{-1} \text{ cm}^{-1}$) for the complexes of H_2L^3 and H_4L^4 , respectively, appeared and probably correspond to ligand-to-metal CT transitions originating from the alcoholate oxygen atom on the central carbon atom. Thus, these data point to the presence of a different chromophore in the $[\text{H}_1\text{LM}]$ species, which probably contains two phosphinate groups and the alcoholate oxygen atoms. The data are similar to those observed for the analogous Cu^{2+} complexes of H_2L^5 and H_2L^6 , for which the coordination of the central alcoholate group was confirmed by solid-state X-ray diffraction.^[23]

X-ray Diffraction Study

During our attempts to crystallize H_2L^2 , single crystals were obtained. Surprisingly, X-ray structure analysis revealed the presence of a polymeric Ca^{2+} complex. The presence of Ca^{2+} ions was confirmed by atomic absorption spectroscopy (AAS) and was explained by the slow leaching of Ca^{2+} ions from the glass vial used during the slow crystallization. The slow complex formation is essential for the growth of single crystals. Any attempts to synthesize the complex directly from Ca^{2+} salts and the ligand led to the precipitation of colloidal solids.

The metal ion was octahedrally coordinated only by the phosphinate oxygen atoms, and the amine group of the ligand was distant and protonated. One of phosphinate groups was disordered with P–O distances of ca. 1.50 Å in the first arrangement and 1.51 and 1.55 Å in the second one (Table S2); this points to the probable protonation of one of the oxygen atoms in the latter case. Indeed, an electronic maximum was present close to the oxygen atom bound to the phosphorus atom with the longest P–O bond, which was attributable to a hydrogen atom. Therefore, the phosphinate group was modelled as disordered in two positions with equal occupancy, one deprotonated, and the other protonated; therefore, H_2L^2 and $(\text{HL}^2)^-$ species are equally abundant. Such a half protonation of the ligand leads to equal abundance of $[(\text{Ca}^{2+})_{0.5}(\text{Cl}^-)_{0.5}\{(\text{H}_2\text{L}^2)\}]^{0.5+}$ and $[(\text{Ca}^{2+})_{0.5}(\text{Cl}^-)_{0.5}\{(\text{HL}^2)^-\}]^{0.5-}$ species and, thus, to the overall formula $[\text{Ca}(\text{H}_2\text{L}^2\text{-}O, O')(\text{HL}^2\text{-}O, O')]\text{Cl}$. The coordination geometry of the Ca^{2+} centre is given in Table S3, and the structure is depicted in Figures 3, S11 and S12. The bisphosphinate groups exhibit two different coordination motifs. The equatorial plane of the octahedron is defined by six-membered chelates formed by two ligands in O, O' -

bidentate mode, that is, one oxygen atom originates from each phosphinate group. This motif is typical for geminal bisphosphonate and bisphosphinate complexes.^[1,34] The other motif is formed by one phosphinate group of each ligand that is simultaneously coordinated to the axial position of a neighbouring metal centre to form a M–O–P–O–M bridge. Two neighbouring metal centres are connected through two of these bridges to form an eight-membered ring, which is typical for solid-state structures of phosphinate complexes.^[35] Both coordination motifs are similar to those found for aminobisphosphonate Ca^{2+} complexes. 4-Amino-1-hydroxybutyl-1,1-bis(phosphonic acid) (alendronate, H_4ale) and 3-amino-1-hydroxypropyl-1,1-bis(phosphonic acid) (pamidronate) form polymeric complexes containing both O, O' -bidentate (one oxygen from each phosphonate) and M–O–P–O–M bridge motifs.^[36] However, the presence of three oxygen atoms on each phosphonate leads to a different overall arrangement of the metal centres and ligand molecules. In addition, 1-hydroxy-1,1-bis(phosphonates) also exhibit tridentate coordination to Ca^{2+} ions through two phosphonates and hydroxy oxygen atoms as has been recently reported for another Ca^{2+} –alendronate complex.^[37] Similarly to our structure, all of the mentioned bisphosphonate complexes also contain a protonated amine group that is not involved in metal-ion coordination.

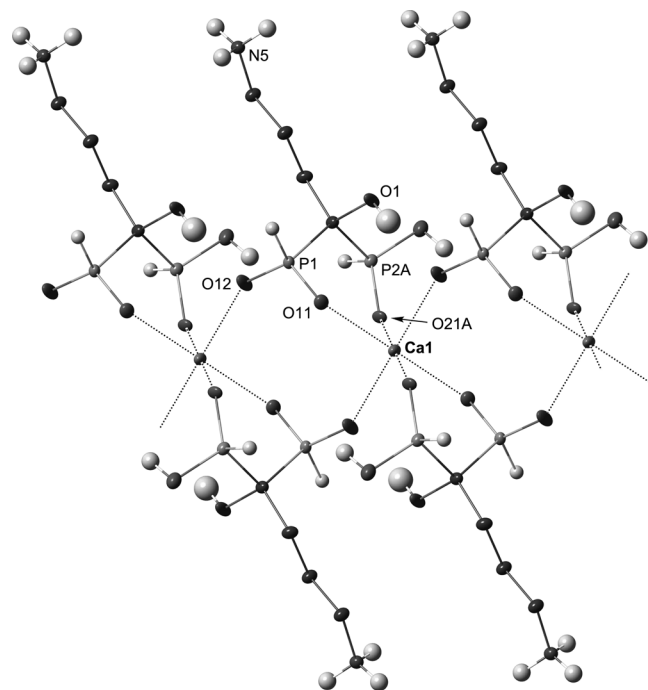


Figure 3. Part of coordination polymer found in the crystal structure of $[\text{Ca}(\text{H}_2\text{L}^2\text{-}O, O')(\text{HL}^2\text{-}O, O')]\text{Cl}$. Of the variants caused by the disorder of the phosphinate function, the one representing the protonated phosphinate $[(\text{Ca}^{2+})_{0.5}(\text{Cl}^-)_{0.5}\{(\text{H}_2\text{L}^2)\}]^{0.5+}$ is shown. Carbon-bound hydrogen atoms are omitted for clarity.

Attempts to crystallize the transition metal complexes studied by potentiometry were mostly unsuccessful owing to the formation of oily or microcrystalline products. We successfully grew single crystals from the Cu^{2+} – H_2L^3 sys-

tem, for which two different solid phases were obtained (depending on the experimental conditions). In the first case [the diffusion of dibenzylamine/*i*PrOH solution into an aqueous $\text{Cu}(\text{NO}_3)_2\text{-H}_2\text{L}^3$ solution to form pale blue crystals], the X-ray diffraction analysis revealed the formula $[\text{Cu}(\text{HL}^3\text{-}O, O')_2(\text{H}_2\text{O})]\cdot 5\text{H}_2\text{O}$. The Cu^{2+} ion is coordinated in an almost regular square-pyramidal coordination sphere ($\tau = 0.05$)^[38] formed by four in-plane oxygen atoms of two different chelating bisphosphinate groups (each oxygen atom originates from a different phosphinate group) and an apically coordinated water molecule (Figures 4 and S13, Table 3). The nitrogen atoms of the ligand molecules are protonated and are away from the coordination sphere. The tetragonal base is slightly distorted with coordination bond lengths $d_{\text{Cu-O}} = 1.93\text{--}1.98 \text{ \AA}$ (Table 3), and the mean difference of the atoms from the average O_4 plane is $\pm 0.022(1) \text{ \AA}$. The Cu-O_{1c} distance to the axial water molecule is ca. 2.25 \AA . The in-plane O-Cu-O angles defined by the oxygen atoms from one ligand molecule are slightly larger (90 and 92° , respectively) than the angles defined by the oxygen atoms from different ligand molecules (ca. 88°). The Cu^{2+} ion is located very close to the tetragonal base; it is only slightly above the O_4 plane by $0.160(1) \text{ \AA}$. The in-plane location of the Cu^{2+} ion mostly predestines the coordination of the sixth donor atom below the basal plane to complete the octahedral sphere. However, surprisingly, there is no such interaction as a result of the geometry of the crystal packing (Figures 5 and S14). The neighbouring complex units are closely packed in the direction of the Cu-O_{1c} coordination bond and do not allow enough space for coordination in the octahedral mode, as there is a short distance (3.40 \AA) between the Cu^{2+} ion and the coordinated water molecule from the neighbouring unit ($x, 1/2 - y, 1/2 + z$), which blocks the sixth position. Water solvate molecules fill the space between the complex units and are located close to the coordinated water molecule. The whole structure is

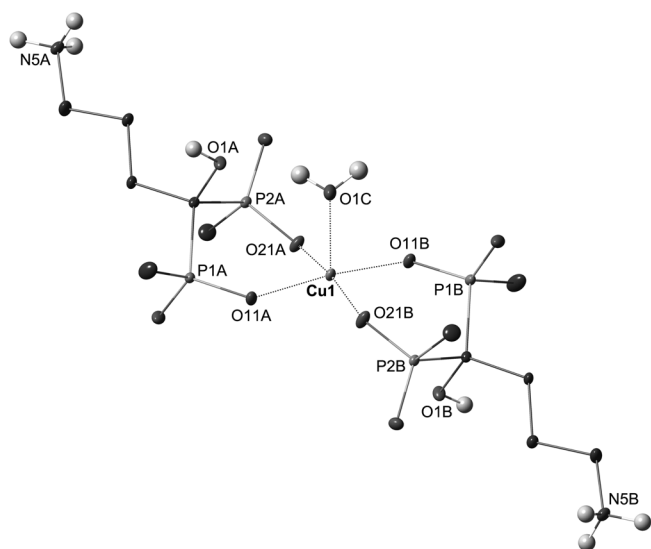


Figure 4. Structure of the $[\text{Cu}(\text{HL}^3\text{-}O, O')_2(\text{H}_2\text{O})]$ complex unit in the crystal structure of $[\text{Cu}(\text{HL}^3\text{-}O, O')_2(\text{H}_2\text{O})]\cdot 5\text{H}_2\text{O}$. Carbon-bound hydrogen atoms are omitted for clarity.

stabilized by a rich network of strong to medium-strong hydrogen bonds between phosphinates, protonated amines, ligand hydroxy groups and water molecules.

Table 3. Geometry of the Cu^{2+} coordination sphere of $[\text{Cu}(\text{HL}^3\text{-}O, O')_2(\text{H}_2\text{O})]\cdot 5\text{H}_2\text{O}$.

Bond lengths [\AA]		Bond angles [$^\circ$]	
Cu1–O1C	2.2457(13)	O1C–Cu1–O11A	92.62(5)
Cu1–O11A	1.9789(11)	O1C–Cu1–O21A	99.81(5)
Cu1–O21A	1.9447(11)	O1C–Cu1–O11B	95.39(5)
Cu1–O11B	1.9784(11)	O1C–Cu1–O21B	90.93(5)
Cu1–O21B	1.9343(12)	O11A–Cu1–O21A	90.33(5)
		O11A–Cu1–O11B	171.98(5)
		O11A–Cu1–O21B	87.91(5)
		O21A–Cu1–O11B	88.03(5)
		O21A–Cu1–O21B	169.18(5)
		O11B–Cu1–O21B	92.24(5)

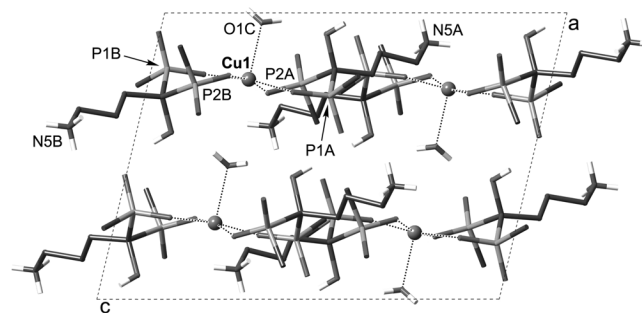


Figure 5. Crystal packing in the solid-state structure of $[\text{Cu}(\text{HL}^3\text{-}O, O')_2(\text{H}_2\text{O})]\cdot 5\text{H}_2\text{O}$; view along the y axis. Solvate water molecules and carbon-bound hydrogen atoms are omitted for clarity.

Similarly to the Ca^{2+} complex, the bisphosphinate coordination mode and geometry in the Cu^{2+} complex resemble those that have been reported for complexes of aminoalkylbisphosphonates. However, the lower number of oxygen atoms results in monomeric bisphosphinate complex, contrary to the bisphosphonates, which mostly form dinuclear complexes or coordination polymers.^[1] The monomeric structure is rather unusual for complexes of simple aminoalkylphosphinates, for which, if the amine group is protonated, the phosphinate group often bridges metal ions to form dimeric or polymeric structural motifs.^[35] On the other hand, the bisphosphinate $\text{H}_2\text{pcp}^{\text{Pb}}$ often forms square-pyramidal Cu^{2+} complexes,^[30,34] which possess both monomeric and polymeric structures, and the Cu-O coordination bonds ($1.9\text{--}2.0 \text{ \AA}$) are of the same length as those found in the structure of $[\text{Cu}(\text{HL}^3\text{-}O, O')_2(\text{H}_2\text{O})]\cdot 5\text{H}_2\text{O}$. Despite their significantly lower basicity, bisphosphinates show Cu-O bond lengths similar to those found in Cu^{2+} complexes of bisphosphonates. This points to the ionic nature of the coordination bonds in complexes of both kinds of ligands.

When a solution of $\text{Cu}^{2+}\text{-H}_2\text{L}^3$ in a water/*i*PrOH mixture was crystallized in the presence of nitrate anions at $\text{pH} \approx 4.5$, light blue-green crystals of a coordination polymer with the formula $[\text{Cu}(\text{H}_{0.5}\text{L}^3\text{-}O, O')(\text{NO}_3)_{0.5}]\cdot 2.25\text{H}_2\text{O}$ were isolated. The structure is polymeric, and, similarly to the previous case, the ligand molecules are coordinated only

Table 4. Geometry of the coordination spheres of both independent Cu²⁺ ions in the structure of [Cu(H_{0.5}L^{3-O,O'})(NO₃)_{0.5}] \cdot 2.25H₂O.

Bond lengths [Å]		Bond angles [°]		Bond angles [°]	
Cu1–O11	1.952(2)	O11–Cu1–O21	93.26(7)	O12–Cu2–O22	94.74(8)
Cu1–O21	1.945(2)	O11–Cu1–O1N	86.04(6)	O12–Cu2–O1N	82.91(7)
Cu1–O1N	2.428(2)	O11–Cu1–O11 ^{#[a]}	180	O12–Cu2–O12 ^{#[b]}	146.1(1)
		O11–Cu1–O21 ^{#[a]}	86.74(7)	O12–Cu2–O22 ^{#[b]}	87.14(8)
Cu2–O12	1.981(2)	O11–Cu1–O1N ^{#[a]}	93.96(6)	O12–Cu2–O1N ^{#[b]}	130.95(7)
Cu2–O22	1.946(2)	O21–Cu1–O1N	90.06(8)	O22–Cu2–O1N	88.95(7)
Cu2–O1N	2.627(2)	O21–Cu1–O21 ^{#[a]}	180	O22–Cu2–O22 ^{#[b]}	173.5(1)
		O21–Cu1–O1N ^{#[a]}	89.94(8)	O22–Cu2–O1N ^{#[b]}	85.14(7)
		O1N–Cu1–O1N ^{#[a]}	180	O1N–Cu2–O12 ^{#[b]}	130.95(7)
				O1N–Cu2–O1N ^{#[b]}	48.04(8)

[a] Symmetry-related atom through centre of symmetry ($2 - x, -y, 2 - z$). [b] Symmetry-related atom through twofold axis ($2 - x, y, 2.5 - z$).

through the phosphinate oxygen atoms. A part of the coordination polymer is shown in Figures 6 and S15. In this structure, two different coordination environments of the copper(II) ions are present. The Cu1 ion is coordinated in a centrosymmetric tetragonal bipyramid elongated by the Jahn–Teller effect with Cu–O axial distances (2.42 Å) significantly longer than the equatorial ones (ca. 1.95 Å). The equatorial sites are occupied by phosphinate oxygen atoms from two ligand molecules, whereas the oxygen atoms of the nitrate anions are bound at the axial sites (Figure 6). The coordination sphere of Cu2 is very irregular, although the Cu centre possesses twofold symmetry. The coordination sphere can be viewed as a trigonal bipyramid with one equatorial position occupied by a bidentate κ -*O,O'*-nitrate ligand with a very long coordination interaction ($d_{\text{Cu-O}} = 2.63$ Å). The other equatorial bonds and the axial bonds are much shorter (1.98 and 1.95 Å, respectively). Selected relevant structural parameters are listed in Table 4. Similarly to the previous structures, the bisphosphinate group is coordinated to each metal centre in *O,O'*-bidentate mode

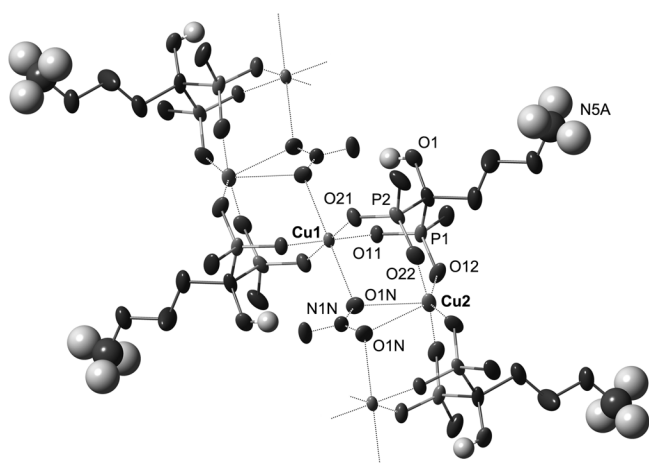


Figure 6. Part of the structure of the complex polymer [Cu(H_{0.5}L^{3-O,O'})(NO₃)_{0.5}] in the crystal structure of [Cu(H_{0.5}L^{3-O,O'})(NO₃)_{0.5}] \cdot 2.25H₂O. Water solvate molecules and carbon-bound hydrogen atoms are omitted for clarity. Of the two disordered positions of the aminopropyl side chain, the one with tentative protonation of the RNH₃⁺ group is shown.

through one oxygen atom from each phosphinate group. Each bisphosphinate group is coordinated to two metal centres in such a chelating mode.

Conclusions

Four geminal bis(phosphinic acids) were synthesized as a new class of chelating ligand. The acids with H–P bonds show limited stability in acidic solutions. The hydrogen atom, which has a somewhat hydride character, behaves as an electron-withdrawing substituent and decreases the stability of the C–P bond in a formally hydrolytic reaction. On the other hand, the presence of other P–C bonds leads to fully stable compounds. The presence of two electron-withdrawing phosphinate groups leads to a low electron density on the adjacent amine group in H₂L¹ and, thus, to the low value of its protonation constant. The same effect leads also to easy metal-assisted deprotonation of the central hydroxy groups in H₂L³ and H₄L⁴, and the alcoholate coordination stabilizes their complexes at neutral and slightly alkaline pH. In connection with our recent results, this phenomenon seems to be general for the coordination properties of ligands with the *P*-hydroxymethyl moiety. The studied bisphosphinates show lower basicity of their amine groups and, thus, less stable complexes with divalent metal ions in comparison with their bisphosphonate analogues. The bisphosphinate moiety forms six-membered chelate rings, which are preferred over the coordination of the weakly basic amine groups. Owing to presence of very acidic phosphinic acid groups, the complexation of the studied metal ions proceeds even at solutions with low pH; this is a highly desirable property in the design of new polydentate ligands for biomedical applications.

Experimental Section

Materials and Methods: Commercially available chemicals had synthetic purity and were used as received. Organic solvents had synthetic purity and were also used as received. Dry CH₂Cl₂ was freshly distilled with P₂O₅. Deionized water was used for synthesis and measurements. [2-(*tert*-Butyloxycarbonyl)ethyl]phosphinic acid was prepared according to the published procedure.^[39] The ¹H, ¹³C

and 2D NMR [H-H COSY, H-C HSQC and H-C HMBC] spectra were recorded at 25 °C with a Bruker Avance III 600 MHz spectrometer equipped with a triple-resonance cold probe. The ^{31}P NMR spectra were recorded at 25 °C with a Varian NMR system operating at 300 MHz proton frequency with an ASW probe. The NMR spectra were referenced to *t*BuOH (internal standard, $\delta_{\text{H}} = 1.25$ ppm, $\delta_{\text{C}} = 30.3$ ppm) and 85% H_3PO_4 (external standard, $\delta_{\text{P}} = 0$ ppm). Chemical shifts are given in ppm, and the coupling constants are given in Hz. ESI-MS spectra were recorded with a Bruker Esquire 3000 spectrometer with ESI ionization and ion-trap detection. TLC was performed with silica on aluminium sheets (Merck 1.0554 F₂₅₄); the spots were detected by UV fluorescence ($\lambda = 254$ nm) or visualized with iodine vapour. Mobile phases for TLC were freshly prepared prior to use.

Aminomethyl-bis(*H*-phosphinic acid) (H_2L^1): Under an argon atmosphere, dry $(\text{NH}_4)_2\text{H}_2\text{PO}_2$ (10.0 g, 120 mmol) was suspended in hexamethyldisilazane (HMDS, 100 mL), and the mixture was heated at 110 °C under a gentle flow of argon overnight. The mixture containing pure $\text{HP}(\text{OTMS})_2$ (TMS = tetramethylsilane) was cooled to r.t., and dry CH_2Cl_2 (100 mL) was added. A suspension of ethyl formimidate hydrochloride (3.31 g, 30.2 mmol) in dry CH_2Cl_2 (150 mL) was added dropwise, and the mixture was stirred at r.t. overnight. Then, the resulting solution was added dropwise into EtOH (500 mL) to hydrolyze the silyl ester groups. The precipitate was collected on a glass frit, and this crude product was purified on a strong cation exchange resin (Dowex 50; H^+ form; elution with water followed by 50% aq. EtOH). The fractions containing the product were combined and evaporated under reduced pressure. The resulting oil was further dried under reduced pressure for several days at r.t. The product was obtained as a colourless oil, which solidified on standing (1.95 g, 37% yield). ^1H NMR ($\text{NaOD}/\text{D}_2\text{O}$, pD 7): $\delta = 2.94$ (t, $^2J_{\text{H,P}} = 15$ Hz, 1 H, CH), 7.08 (d, $^1J_{\text{H,P}} = 541$ Hz, 2 H, PH) ppm. $^{13}\text{C}\{^1\text{H}\}$ NMR: $\delta = 54.4$ (t, $^1J_{\text{C,P}} = 80$ Hz, CH) ppm. ^{31}P NMR: $\delta = 17.0$ (dm, $^1J_{\text{P,H}} = 541$ Hz) ppm. MS (-): $m/z = 158.6$ [$\text{M} - \text{H}$] $^-$. MS (+): $m/z = 160.7$ [$\text{M} + \text{H}$] $^+$. TLC (MeCN/MeOH/conc. aq. NH_3 3:1:2): $R_f = 0.2$. $\text{CH}_7\text{NO}_4\text{P}_2$ (159.0): calcd. C 7.6, H 4.4, N 8.8; found C 7.8, H 4.5, N 8.7.

Aminomethyl-(*H*-phosphinic acid) (III): In a glass vial, H_2L^1 (40.1 mg; 252 μmol) was dissolved in 1 M aq. HCl (0.5 mL), and the mixture was heated at 80 °C for 2 d. After cooling to r.t., the mixture was evaporated to dryness. The residue was dissolved in water (0.5 mL), and *i*PrOH (3.0 mL) was then added to produce a cloudy mixture. The mixture was refrigerated overnight, and the upper phase was discarded; the resulting oil was purified on a strong cation exchange resin (Dowex 50; H^+ form; elution with water followed by 10% aq. pyridine). The pyridine fraction was evaporated to dryness and coevaporated with water several times. The resulting oily product (^{31}P NMR purity > 95%) was characterized without further purification or isolation. ^1H NMR (D_2O , pD 4): $\delta = 3.04$ (d, $^2J_{\text{H,P}} = 11$ Hz, 2 H, CH_2), 7.08 (d, $^1J_{\text{H,P}} = 541$ Hz, 1 H, PH) ppm. $^{13}\text{C}\{^1\text{H}\}$ NMR: $\delta = 39.3$ (d, $^1J_{\text{C,P}} = 89$ Hz, CH_2) ppm. ^{31}P NMR: $\delta = 14.5$ (dt, $^1J_{\text{P,H}} = 541$ Hz, $^2J_{\text{P,H}} = 11$ Hz) ppm. MS (-): $m/z = 94.2$ [$\text{M} - \text{H}$] $^-$. TLC (MeCN/MeOH/conc. aq. NH_3 3:1:2): $R_f = 0.6$.

4-(Phthalimido)butanoyl Chloride (IV): In a 50 mL flask, 4-(phthalimido)butanoic acid (3.79 g, 15.1 mmol) was dissolved in CH_2Cl_2 (25 mL), and $(\text{COCl})_2$ (3.20 mL, 37.5 mmol) was added. The resulting mixture was stirred at r.t. for 3 h and then evaporated to dryness. The residue was coevaporated three times with dry CH_2Cl_2 and then dissolved in dry CH_2Cl_2 (10 mL). The solution was used immediately as obtained in the next reactions.

4-Amino-1-hydroxybutyl-1,1-bis(*H*-phosphinic acid) (H_2L^2): Under an argon atmosphere, dry $(\text{NH}_4)_2\text{H}_2\text{PO}_2$ (5.00 g, 60.2 mmol) was

suspended in HMDS (50 mL), and the mixture was heated at 110 °C under a gentle flow of argon overnight. The mixture containing pure $\text{HP}(\text{OTMS})_2$ was cooled to r.t., and dry CH_2Cl_2 (25 mL) was added. Then, a freshly prepared solution of **IV** obtained from 4-(phthalimido)butanoic acid (3.79 g, 15.1 mmol) was added, and the mixture was stirred at r.t. overnight. Then, the resulting solution was added dropwise into EtOH (200 mL) to hydrolyze the silyl ester groups. The precipitate was collected on a glass frit and washed with EtOH (50 mL). Another fraction of the solid was collected from the filtrate after it had stood overnight. Both fractions were combined and dried with P_2O_5 in a vacuum desiccator. The crude 4-(phthalimido)butyl-1,1-bis(*H*-phosphinic acid) (**Va**) was obtained as a white powder (5.85 g) and was not further purified. The crude **Va** was dissolved in a mixture of 75% aq. N_2H_4 (60 mL) and EtOH (60 mL), and the solution was stirred at r.t. overnight. An excess of EtOH (300 mL) was then added, and the flask was refrigerated for 3 d. The upper phase was decanted; the resulting oil was dissolved in water (40 mL), and EtOH (300 mL) was added. The next day, the upper phase was decanted, and the remaining oil was dissolved in conc. aq. ammonia (100 mL), evaporated to dryness and further coevaporated three times with water. The residue was dissolved in water (100 mL), and the resulting solution was adjusted to pH 8 with 2 M aq. NaOH. The solution was evaporated to dryness, the residue was dissolved in water (100 mL), and the solution was again adjusted to pH 8 with 2 M aq. NaOH. This procedure was repeated until the redissolved aq. solution reached pH 8. Then, the solution was concentrated to 10 mL and slowly added dropwise into a vigorously stirred mixture of anhydrous EtOH/tetrahydrofuran (EtOH/THF, 1:1, 400 mL). The precipitate was collected on a glass frit and washed with MeOH (200 mL). The resulting solid was dissolved in water (100 mL), and some charcoal was added. The mixture was filtered, and the filtrate was evaporated to dryness and further coevaporated several times with water (100 mL). The resulting solid was dried with P_2O_5 in a vacuum desiccator. The product was obtained as a white crystalline powder as a mixed ammonium-sodium salt (2.29 g, 54%). ^1H NMR (D_2O , pD 7): $\delta = 1.90$ (m, 2 H, CH_2CP), 1.99 (m, 2 H, $\text{CH}_2\text{CH}_2\text{N}$), 3.05 (t, $^3J_{\text{H,H}} = 7$ Hz, 2 H, CH_2N), 6.96 (dt, $^1J_{\text{H,P}} = 527$ Hz, $^3J_{\text{H,P}} = 17$ Hz, 2 H, PH) ppm. $^{13}\text{C}\{^1\text{H}\}$ NMR: $\delta = 23.6$ (t, $^2J_{\text{C,P}} = 6$ Hz, CH_2CP), 29.5 (s, CH_2CN), 42.2 (s, CH_2N), 75.8 (t, $^1J_{\text{C,P}} = 93$ Hz, CP) ppm. ^{31}P NMR: $\delta = 24.5$ (dm, $^1J_{\text{P,H}} = 527$ Hz) ppm. $^{31}\text{P}\{^1\text{H}\}$ NMR: $\delta = 24.5$ (s) ppm. MS (-): $m/z = 215.4$ [$\text{M} - \text{H}$] $^-$. TLC (EtOH/conc. aq. NH_3 1:1): $R_f = 0.3$. $\text{Na}_{1.6}(\text{NH}_4)_{0.4}\text{C}_4\text{H}_{11}\text{NO}_5\text{P}_2 \cdot 0.5\text{H}_2\text{O}$ (282.2): calcd. C 17.0, H 4.7, N 6.9; found C 17.2, H 4.8, N 6.7.

4-Amino-1-hydroxybutyl-1-(*H*-phosphinic acid) (VI): In a glass vial, H_2L^2 (300 mg, 1.06 mmol) was dissolved in 1 M aq. HCl (5 mL), and the mixture was heated at 80 °C for 30 d. After cooling to r.t., the mixture was evaporated to dryness. The crude product was purified on a strong cation exchange resin (Dowex 50; H^+ form; elution with water followed by 10% aq. pyridine). The pyridine fraction was evaporated to dryness and coevaporated with water several times. The resulting oily product (94% purity as determined by ^{31}P NMR spectroscopy) was analyzed without further purification.

^1H NMR (D_2O , pD 4): $\delta = 1.64$ (m, 1 H, CH_2CP), 1.79 (m, 1 H, CH_2CP), 1.79 (m, 1 H, $\text{CH}_2\text{CH}_2\text{N}$), 1.93 (m, 1 H, $\text{CH}_2\text{CH}_2\text{N}$), 3.06 (m, 2 H, CH_2N), 3.58 (m, 1 H, CHP), 6.79 (dm, $^1J_{\text{H,P}} = 509$ Hz, 1 H, PH) ppm. $^{13}\text{C}\{^1\text{H}\}$ NMR: $\delta = 24.1$ (d, $^3J_{\text{C,P}} = 12$ Hz, $\text{CH}_2\text{CH}_2\text{N}$), 26.7 (s, CH_2CP), 39.9 (s, CH_2N), 70.3 (d, $^1J_{\text{C,P}} = 109$ Hz, CP) ppm. ^{31}P NMR: $\delta = 29.1$ (d, $^1J_{\text{P,H}} = 509$ Hz) ppm. $^{31}\text{P}\{^1\text{H}\}$ NMR: $\delta = 29.15$ (s) ppm. MS (-): $m/z = 152.0$ [$\text{M} - \text{H}$] $^-$.

MS (+): $m/z = 154.2$ [M + H]⁺. TLC (EtOH/conc. aq. NH₃ 1:1): $R_f = 0.5$.

4-Amino-1-hydroxybutyl-1,1-bis(methyl)phosphinic acid (H₂L³): In a 100 mL flask, *N*-ethyl-diisopropylamine (DIPEA, 12.0 mL, 68.8 mmol) was added to a solution of methylphosphinic acid (2.21 g, 27.6 mmol) in dry CH₂Cl₂ (25 mL). Subsequently, chlorotrimethylsilane (TMSCl, 8.80 mL, 69.0 mmol) was slowly added, and the resulting mixture was stirred at r.t. for 3 h. Then, a freshly prepared solution of **IV** obtained from 4-(phthalimido)butanoic acid (2.78 g, 11.1 mmol) was added, and the mixture was stirred at r.t. overnight. Ethanol (50 mL) was then slowly added to the reaction mixture to hydrolyze the silyl ester groups. The resulting solution was evaporated to dryness and then coevaporated with CH₂Cl₂. The residue was dissolved in 2 M aq. NaOH (50 mL) and extracted with CH₂Cl₂ (4 × 50 mL). The aqueous phase was evaporated to dryness, and the residue was purified on a strong cation exchange resin (Dowex 50, H⁺ form, elution with water), and the eluate was evaporated to dryness. The resulting mixture was dissolved in 6 M aq. HCl (100 mL) and heated to reflux for 3 d. Then, the reaction mixture was cooled to r.t. After 3 h, the precipitated phthalic acid was removed by filtration, and the filtrate was evaporated to dryness. The residue was dissolved in a mixture of THF/MeOH/water (2:1:2, 5 mL) and purified by column chromatography [SiO₂; elution with THF/MeOH/conc. aq. NH₃ 2:1:2 followed by 1:1:2; R_f (product) = 0.1 → 0.4]. The fractions containing the pure product were combined, and the solvents were evaporated to dryness. The ammonia was removed from the crude product on a strong cation exchange resin (Dowex 50, H⁺ form, elution with water followed by 10% aq. pyridine). The pyridine fraction was evaporated to dryness and coevaporated several times with water. The residual pyridine was removed on a weak cation exchange resin (Amberlite CG50, H⁺ form, water elution). The fractions containing the product were combined, and the solvents were evaporated to dryness. The resulting solid was dried with P₂O₅ in a vacuum desiccator. The product was obtained as a white powder (1.81 g, 60%). ¹H NMR (D₂O, pD 6): $\delta = 1.38$ (m, 6 H, CH₃), 2.01 (m, 4 H, CH₂CH₂N and CH₂CO), 3.04 (t, ³J_{H,H} = 7 Hz, 2 H, CH₂N) ppm. ¹³C{¹H} NMR: $\delta = 16.9$ (m, CH₃), 24.4 (s, CH₂CO), 31.9 (s, CH₂CH₂N), 42.5 (s, CH₂N), 77.8 (t, ¹J_{C,P} = 93 Hz, CP) ppm. ³¹P{¹H} NMR: $\delta = 39.9$ (s) ppm. MS (-): $m/z = 243.7$ [M - H]⁻, 488.8 [2M - H]⁻. TLC (THF/MeOH/conc. aq. NH₃ 1:1:2): $R_f = 0.4$. C₆H₁₇NO₅P₂·1.5H₂O (272.2): calcd. C 26.5, H 7.4, N 5.2; found C 26.7, H 7.0, N 5.5.

4-Amino-1-hydroxybutyl-1,1-bis(2-carboxyethyl)phosphinic acid (H₄L⁴): In a 50 mL flask, DIPEA (7.21 mL, 41.4 mmol) was added to a solution of [2-(*tert*-butyloxycarbonyl)ethyl]phosphinic acid (1.34 g, 6.90 mmol) in dry CH₂Cl₂ (10 mL). Subsequently, TMSCl (5.25 mL, 41.4 mmol) was slowly added, and the resulting mixture was stirred at r.t. for 3 h. Then, a freshly prepared solution of **IV** obtained from 4-(phthalimido)butanoic acid (600 mg, 2.57 mmol) was added, and the mixture was stirred at r.t. overnight. Ethanol (20 mL) was then slowly added to the reaction mixture to hydrolyze the silyl ester groups. The resulting solution was evaporated to dryness and then coevaporated with CH₂Cl₂. The residue was dissolved in 3% aq. HCl (30 mL) and extracted with CH₂Cl₂ (5 × 15 mL). The organic layers were combined, and the solvents were evaporated to dryness. The crude compound **Vc** was dissolved in a mixture of N₂H₄ (75% aq. solution, 20 mL) and EtOH (20 mL), and the mixture was stirred at r.t. for 3 d. An excess of EtOH (100 mL) was then added, and the mixture was refrigerated overnight. The upper phase was decanted, and the resulting oil was purified on a strong anion exchange resin (Dowex 1, OH⁻ form, elution with water followed by 20% and 50% aq. AcOH). The

product-containing fractions (eluted with 50% aq. AcOH) were combined, evaporated to dryness and further coevaporated with water. The resulting solid was dried with P₂O₅ in a vacuum desiccator. The product was obtained as a white hygroscopic powder (486 mg, 49%). ¹H NMR (D₂O, pD 2): $\delta = 2.03$ (m, 4 H, CH₂CH₂N and CH₂COH), 2.16 (m, 4 H, CH₂P), 2.67 (m, 4 H, CH₂CO₂H), 3.05 (t, ³J_{H,H} = 7 Hz, 2 H, CH₂N) ppm. ¹³C{¹H} NMR: $\delta = 24.4$ (s, CH₂COH), 23.3 (m, CH₂P), 27.4 (s, CH₂C₂H), 30.1 (s, CH₂CH₂N), 40.5 (s, CH₂N), 76.0 (t, ¹J_{C,P} = 92 Hz, CP), 178.2 (d, ³J_{C,P} = 15 Hz, CO) ppm. ³¹P{¹H} NMR: $\delta = 44.4$ (s) ppm. MS (-): $m/z = 359.1$ [M - H]⁻. MS (+): $m/z = 361.2$ [M + H]⁺, 383.4 [M + Na]⁺, 399.2 [M + K]⁺. TLC (THF/MeOH/conc. aq. NH₃ 2:1:2): $R_f = 0.2$. C₁₀H₂₁NO₉P₂·1.5H₂O (388.2): calcd. C 30.9, H 6.2, N 3.6; found C 30.7, H 5.8, N 3.9.

The fractions eluted from the strong anion exchange resin with 20% aq. AcOH contained a side-product (ca. 30% yield), which was identified as the hydrazide of H₄L⁴ (for the structure, see Figure S1). ¹H NMR (D₂O, pD 2): $\delta = 1.90$ –2.23 (m, 8 H, CH₂CH₂N, CH₂COH, CH₂P), 2.56–2.73 (m, 4 H, CH₂COOH), 3.05 (m, 2 H, CH₂N) ppm. ¹³C{¹H} NMR: $\delta = 22.5$ (CH₂COH, s), 23.1–24.3 (m, CH₂P), 26.8 (s, CH₂CO), 27.6 (s, CH₂CO), 30.2 (m, CH₂CH₂N), 40.6 (s, CH₂N), 76.3 (t, ¹J_{C,P} = 93 Hz, CP), 174.5 (d, ³J_{C,P} = 13 Hz, CONH), 178.6 (d, ³J_{C,P} = 14 Hz, COOH) ppm. ³¹P{¹H} NMR: $\delta = 41.2$ (d, ²J_{P,P} = 28 Hz, 1 P), 42.9 (d, ²J_{P,P} = 28 Hz, 1 P) ppm. MS (-): $m/z = 374.3$ [M - H]⁻. MS (+): $m/z = 375.9$ [M + H]⁺. TLC (THF/MeOH/conc. aq. NH₃ 2:1:2): $R_f = 0.3$.

Kinetics of Hydrolysis: The hydrolyses of H₂L¹ and H₂L² at concentrations of 10 mM were followed by ³¹P NMR spectroscopy. The experiments were performed at constant temperature (80 °C) maintained by a thermostatted bath or by the NMR spectrometer. The experiments were performed in 1 M aq. HCl (pH 0) or 1 M aq. NaOH (pH 14).

Potentiometric Titrations: The methodology of the potentiometric titrations and processing of the experimental data were analogous to those previously reported.^[40] The titrations were performed in a vessel thermostatted at (25 ± 0.1) °C with solutions of ionic strength $I = 0.1$ M KNO₃. The ligand-to-metal ratios were 1:1 and 2:1 (as well as 1:2 for H₄L⁴) with $c_L = 0.004$ M; the pH range was 1.7–12 (or until metal hydroxide precipitated). The titrations were performed at least three times, and each consisted of ca. 40 points. The water ion product ($pK_w = 13.78$) and the stability constants of the M²⁺-OH⁻ systems were taken from ref.^[41] The calculated protonation constants β_n are concentration constants and are defined by $\beta_n = [H_nL]/([H]^n[L])$; $\log K_1 = \log \beta_1$ and $\log K_n = \log \beta_n - \log \beta_{n-1}$. The overall stability constant are defined by $\beta_{hlm} = [M_nH_hL_l]/([M]^n[H]^h[L]^l)$. The constants (with standard deviations) were calculated with the program OPIUM.^[42] Throughout the paper, pH means $-\log[H^+]$.

NMR Titrations: The ³¹P{¹H} and ¹H NMR titration experiments to determine the nitrogen protonation constants of H₂L¹ and H₂L² (pH 4–13, ca. 15 points) were performed without control of ionic strength at 25.0 °C and ligand concentration $c_L = 0.004$ M. A coaxial capillary tube with D₂O and H₃PO₄ was used for the lock signal and referencing. The pH values of the samples were adjusted with 0.1 M aq. HCl or 0.1 M aq. NaOH. The protonation constants were obtained with the software OPIUM^[40] by simultaneous treatment of ¹H and ³¹P NMR spectroscopic data. The overlap of both ¹H NMR signals in the P-C-CH₂-CH₂ fragment of H₂L² disabled the precise analysis and, thus, only the signal of the methylene group attached to the amine group was used for evaluation of the data.

UV/Vis Measurements: UV/Vis spectra were measured with a Shimadzu UV-2401PC spectrometer at 25 °C in the wavelength range

200–900 nm. Solutions of ligand and metal ions were mixed, and the pH was adjusted to the desired value by the addition of 0.1 M aq. HCl or 0.1 M aq. NaOH. Then, the samples were diluted with water to reach a final metal concentration $c_M = 5$ mM for measurements in the visible region or $c_M = 0.5$ mM for measurements in the UV region.

X-ray Diffraction: A few single crystals of $[\text{Ca}(\text{H}_2\text{L}^2\text{-O},\text{O}')(\text{HL}^2\text{-O},\text{O}')]\text{Cl}$ were obtained by long time (1 month) standing of a closed vial containing a mixture of H_2L^2 (18.5 mg, mixed sodium ammonium salt), 3% aq. HCl (160 μL), *i*PrOH (400 μL) and water (200 μL). The source of calcium is probably the glass of the vial; its presence in the mother solution was confirmed by AAS analysis.

Single crystals of $[\text{Cu}(\text{HL}^3\text{-O},\text{O}')_2(\text{H}_2\text{O})]\cdot 5\text{H}_2\text{O}$ were obtained by slow diffusion of a 4% dibenzylamine solution in *i*PrOH (1 mL) into a solution of H_2L^3 (19.5 mg, 71.6 μmol) and $\text{Cu}(\text{NO}_3)_2\cdot 6\text{H}_2\text{O}$ (9.6 mg, 32.6 μmol) in water (0.5 mL).

Single crystals of $[\text{Cu}(\text{H}_{0.5}\text{L}^3\text{-O},\text{O}')(\text{NO}_3)_{0.5}]\cdot 2.25\text{H}_2\text{O}$ were prepared by mixing H_2L^3 (19.6 mg, 72.0 μmol), $\text{Cu}(\text{NO}_3)_2\cdot 6\text{H}_2\text{O}$ (19.3 mg, 65.5 μmol) and picric acid (16.5 mg, 72.0 μmol) in water (0.5 mL). Guanidinium carbonate was added until all solid dissolved (pH \approx 4.5), and the mixture was briefly heated at 80 °C. A blue powder formed over a few weeks and was collected by filtration, dissolved in water (0.5 mL) and crystallized by the addition *i*PrOH (0.5 mL). The complex also formed in the absence of picric acid and guanidinium carbonate; however, the single crystals were of low quality.

The diffraction data were collected at 150 K (Cryostream Cooler, Oxford Cryosystem) by using a Nonius Kappa CCD diffractometer and Mo- K_α radiation ($\lambda = 0.71073$ Å). The frames were integrated with the Bruker SAINT software package by using a narrow-frame algorithm.^[43] The data were corrected for absorption effects by using the multiscan method (SADABS).^[44] The structures were solved by direct methods (SHELXS97)^[45] and refined by full-matrix least-squares techniques (SHELXL97).^[46] All non-hydrogen atoms were refined anisotropically. All hydrogen atoms were located in the electron density difference map; however, they were placed in theoretical (C–H, N–H) or original (O–H) positions with

thermal parameters $U_{\text{eq}}(\text{H}) = 1.2U_{\text{eq}}(\text{X})$, as their free refinement led to several unrealistic bond lengths. For the crystal structure of $[\text{Ca}(\text{H}_2\text{L}^2\text{-O},\text{O}')(\text{HL}^2\text{-O},\text{O}')]\text{Cl}$, the independent unit is formed by Ca, Cl and one ligand molecule, and the Ca and Cl atoms are in special positions with half occupancy. The amine group of the ligand is protonated. One of phosphinate functions was found to be disordered and was modelled in two positions with equal occupancy (Figure S11). In one possibility, the phosphinate function is protonated, whereas in the second possibility it is not, as documented also by the P–O bond lengths (Table S2). Such half protonation is a result of a need to compensate the overall charge of the Ca^{2+} and Cl^- ions and results in the formal formula $(\text{Ca}^{2+})_{0.5}(\text{Cl}^-)_{0.5}\cdot \{(\text{H}_{1.5}\text{L}^2)^{0.5-}\}$, that is, $[\text{Ca}(\text{H}_2\text{L}^2\text{-O},\text{O}')(\text{HL}^2\text{-O},\text{O}')]\text{Cl}$. For $[\text{Cu}(\text{HL}^3\text{-O},\text{O}')_2(\text{H}_2\text{O})]\cdot 5\text{H}_2\text{O}$, no special treatment was needed. For $[\text{Cu}(\text{H}_{0.5}\text{L}^3\text{-O},\text{O}')(\text{NO}_3)_{0.5}]\cdot 2.25\text{H}_2\text{O}$, the independent unit is formed by one ligand molecule, two half-occupied copper(II) ions, a half-occupied nitrate anion and some solvate water molecules. The ligand oxygen atoms are deprotonated and coordinated to Cu^{2+} ions, and the ligand hydroxy group was clearly found to be protonated. Therefore, the ligand molecule must be partially protonated by 0.5H on the side amine group to ensure electroneutrality of the overall formula. This is probably a reason for the observed disorder of the aliphatic part of the molecule; therefore, this disorder was modelled by splitting the side chain over two positions with half occupancy. However, although some maxima in the electron difference map could be attributed to hydrogen atoms, not all hydrogen atoms could be located (as the disorder is probably more complicated) and, therefore, the hydrogen atoms were placed in theoretical or original positions by using a riding model. The amine group in one of the two positions was tentatively declared as protonated, and the AFIX 137 instruction was used; the protons of the second half of the amine group were located in the electronic map. In the cavities of the polymeric complex framework, some maxima of electron density were found in the free space between the polymeric chains and attributed to solvate water molecules. However, their mutual geometry and low intensities point to a complicated disorder, which was modelled by their attribution to water molecules with 0.25–0.5 occupancy. This resulted in more than two H_2O molecules per formula unit, but a number of small maxima

Table 5. Experimental data of reported crystal structures.

	$[\text{Ca}(\text{H}_2\text{L}^2\text{-O},\text{O}')(\text{HL}^2\text{-O},\text{O}')]\text{Cl}$	$[\text{Cu}(\text{HL}^3\text{-O},\text{O}')_2(\text{H}_2\text{O})]\cdot 5\text{H}_2\text{O}$	$[\text{Cu}(\text{H}_{0.5}\text{L}^3\text{-O},\text{O}')(\text{NO}_3)_{0.5}]\cdot 2.25\text{H}_2\text{O}$
Formula	$\text{C}_8\text{H}_{25}\text{CaClN}_2\text{O}_{10}\text{P}_4$	$\text{C}_{12}\text{H}_{44}\text{CuN}_2\text{O}_{16}\text{P}_4$	$\text{C}_6\text{H}_{20}\text{CuN}_{1.5}\text{O}_{8.75}\text{P}_2$
M_w	508.71	659.91	378.71
Colour	colourless	light blue	light blue-green
Shape	prism	prism	prism
Dimensions [mm]	$0.105 \times 0.203 \times 0.261$	$0.287 \times 0.405 \times 0.421$	$0.265 \times 0.276 \times 0.379$
Crystal system	monoclinic	monoclinic	monoclinic
Space group	$C2/c$	$P2_1/c$	$C2/c$
a [Å]	23.6965(11)	15.5110(2)	14.8708(3)
b [Å]	5.2028(2)	16.1990(2)	17.7541(4)
c [Å]	18.4274(8)	11.2788(2)	12.8882(4)
β [°]	119.639(2)	103.428(1)	124.8959(8)
V [Å ³]	1974.62(15)	2756.47(7)	2790.87(12)
Z	4	4	8
$D_{\text{calcd.}}$ [g cm ⁻³]	1.711	1.590	1.803
μ [mm ⁻¹]	0.826	1.093	1.833
$F(000)$	1056	1388	1564
Diffractions, observed [$I_0 > 2\sigma(I_0)$]	2266, 2017	6338, 5660	3202, 2841
Parameters	130	328	190
GoF on F^2	1.078	1.053	1.110
R, R' (all data)	0.0297, 0.0346	0.0266, 0.0306	0.0342, 0.0379
wR, wR' (all data)	0.0790, 0.0823	0.0763, 0.0792	0.0968, 0.0995
Difference max., min. (e Å ⁻³)	0.534, -0.385	0.963, -0.493	0.854, -0.594

still remained close to these partially occupied water molecules, which points to a very complicated disorder. Therefore, all solvent-related maxima were squeezed by using PLATON.^[47] The squeezed electronic intensity (2.25H₂O) corresponds well to previous findings. Selected crystallographic parameters for the reported structures are listed in Table 5.

CCDC-983603 {for [Ca(H₂L²-O,O')(HL²-O,O')]Cl}, -983601 {for [Cu(HL³-O,O')₂(H₂O)]·5H₂O} and -983602 {for [Cu(H_{0.5}L³-O,O')(NO₃)_{0.5}]·2.25H₂O} contain the supplementary crystallographic data for this paper. These data can be obtained free of charge from The Cambridge Crystallographic Data Centre via www.ccdc.cam.ac.uk/data_request/cif.

Supporting Information (see footnote on the first page of this article): Coordination polymer motif in the crystal structure of [Ca(H₂L²-O,O')(HL²-O,O')]Cl; geometric parameters of phosphinate functions in the crystal structure of [Ca(H₂L²-O,O')(HL²-O,O')]Cl; time course of decomposition of H₂L¹ and H₂L² in acidic solution; ³¹P and ¹H NMR titrations of H₂L¹ and H₂L²; determined equilibrium constants; distribution diagrams of the studied metal–ligand systems; geometry of the Ca²⁺ coordination sphere of [Ca(H₂L²-O,O')(HL²-O,O')]Cl; structure of the hydrazide isolated as a side-product of the synthesis of H₄L⁴; and colour figures of the solid-state structures of the complexes.

Acknowledgments

Support from the Grant Agency of the Czech Republic (grant number P207/10/P153), the Grant Agency of the Charles University (grant number 310011) and the Ministry of Education of the Czech Republic (Long-Term Research Plan, grant number MSM0021620857) is acknowledged. This work was further supported by the European Union (EU) and carried out within the framework of COST Actions TD1004, TD1007 and CM1006 (MSMT number LD 13012). The authors thank Dr. Jakub Hraníček for AAS measurements.

- [1] E. Matczak-Jon, V. Videnova-Adrabinska, *Coord. Chem. Rev.* **2005**, *249*, 2458–2488.
- [2] C. Queffelec, M. Petit, P. Janvier, D. A. Knight, B. Bujoli, *Chem. Rev.* **2012**, *112*, 3777–3807.
- [3] G. Guerrero, J. G. Alauzun, M. Granier, D. Laurencin, P. H. Mutin, *Dalton Trans.* **2013**, *42*, 12569–12585.
- [4] A. Mucha, P. Kafarski, L. Berlicki, *J. Med. Chem.* **2011**, *54*, 5955–5980.
- [5] A. Vioux, J. Le Bideau, P. H. Mutin, D. Leclercq, *Top. Curr. Chem.* **2004**, *232*, 145–174.
- [6] I. Řehoř, V. Kubiček, J. Kotek, P. Hermann, J. Száková, I. Lukes, *Eur. J. Inorg. Chem.* **2011**, 1981–1989.
- [7] M. de los Reyes, P. J. Majewski, N. Scales, V. Luca, *ACS Appl. Mater. Interfaces* **2013**, *5*, 4120–4128.
- [8] D. Portet, B. Denizot, E. Rump, J.-J. Lejeune, P. Jallet, *J. Colloid Interface Sci.* **2001**, *238*, 37–42.
- [9] A. Panahifar, M. Mahmoudi, M. R. Doschak, *ACS Appl. Mater. Interfaces* **2013**, *5*, 5219–5226.
- [10] L. Sandiford, A. Phinikaridou, A. Protti, L. K. Meszaros, X. Cui, Y. Yan, G. Frodsham, P. A. Williamson, N. Gaddum, R. M. Botnar, P. J. Blower, M. A. Green, R. T. M. de Rosales, *ACS Nano* **2013**, *7*, 500–512.
- [11] Y. Lalatonne, C. Paris, J.-M. Serfaty, P. Weinmann, M. Lecouvey, L. Motte, *Chem. Commun.* **2008**, 2553–2555.
- [12] V. Kubiček, I. Lukeš, *Future Med. Chem.* **2010**, *2*, 521–531.
- [13] E. Palma, J. D. G. Correia, M. P. C. Campello, I. Santos, *Mol. Biosyst.* **2011**, *7*, 2950.
- [14] J. Galezowska, E. Gumienka-Konteckab, *Coord. Chem. Rev.* **2012**, *256*, 105–124.
- [15] E. V. Giger, B. Castagner, J.-C. Leroux, *J. Controlled Release* **2013**, *167*, 175–188.
- [16] a) G. A. Rodan, H. A. Fleisch, *J. Clin. Invest.* **1996**, *97*, 2692–2696; b) H. Fleisch, *Endocr. Rev.* **1998**, *19*, 80–100.
- [17] S. P. Luckman, F. P. Coxon, F. H. Ebetino, R. G. G. Russell, M. J. Rogers, *J. Bone Miner. Res.* **1998**, *13*, 1668–1678.
- [18] T. David, P. Křečková, J. Kotek, V. Kubiček, I. Lukeš, *Heteroat. Chem.* **2012**, *23*, 195–201.
- [19] a) S. Gouault-Bironneau, S. Deprele, A. Sutor, J.-L. Montchamp, *Org. Lett.* **2005**, *7*, 5909–5912; b) M. I. Antczak, J.-L. Montchamp, *Tetrahedron Lett.* **2008**, *49*, 5909–5913.
- [20] B. Kaboudin, F. Saadati, T. Yokomatsu, *Synlett* **2010**, 1837–1840.
- [21] M. Bochno, Ł. Berlicki, *Tetrahedron Lett.* **2014**, *55*, 219–22.
- [22] a) F. Gaizer, G. Haegle, S. Goudetsidis, H. Papadopoulos, Z. *Naturforsch. B* **1990**, *45*, 323–328; b) L. P. Loginova, I. V. Levin, A. G. Matveeva, S. A. Pisareva, E. E. Nifantev, *Russ. Chem. Bull.* **2004**, *53*, 2000–2007.
- [23] T. David, S. Procházková, J. Havlíčková, J. Kotek, V. Kubiček, P. Hermann, I. Lukeš, *Dalton Trans.* **2013**, *42*, 2414–2422.
- [24] A. A. Prishchenko, M. V. Livantsov, O. P. Novikova, L. I. Livantsova, *Russ. J. Gen. Chem.* **2010**, *80*, 1889–1890.
- [25] K. Issleib, W. Moegelin, A. Balszuweit, *Z. Chem.* **1985**, *25*, 370–371.
- [26] a) E. K. Baylis, C. D. Campbell, J. G. Dingwall, *J. Chem. Soc. Perkin Trans. 1* **1984**, 2845–2853; b) J. Rohovec, I. Lukeš, P. Vojtišek, I. Cisařová, P. Hermann, *J. Chem. Soc., Dalton Trans.* **1996**, 2685–2691.
- [27] J. Kehler, B. Ebert, O. Dahl, P. Krosggaard-Larsen, *Tetrahedron* **1999**, *55*, 771–780.
- [28] V. Kubiček, J. Kotek, P. Hermann, I. Lukeš, *Eur. J. Inorg. Chem.* **2007**, 333–344.
- [29] I. Lukeš, J. Kotek, P. Vojtišek, P. Hermann, *Coord. Chem. Rev.* **2001**, *216–217*, 287–312.
- [30] S. Ciattini, F. Costantino, P. Lorenzo-Luis, S. Midollini, A. Orlandini, A. Vacca, *Inorg. Chem.* **2005**, *44*, 4008–4016.
- [31] J. Šimeček, P. Hermann, J. Havlíčková, E. Herdtweck, T. G. Kapp, N. Engelbogen, H. Kessler, H.-J. Wester, J. Notni, *Chem. Eur. J.* **2013**, *19*, 7748–7757.
- [32] J. Šimeček, O. Zemek, P. Hermann, J. Notni, H.-J. Wester, *Mol. Pharmaceutics*, DOI: 10.1021/mp400642s.
- [33] J. Šimeček, M. Schulz, J. Notni, J. Plutnar, V. Kubiček, J. Havlíčková, P. Hermann, *Inorg. Chem.* **2012**, *51*, 577–590.
- [34] a) J. Beckmann, F. Costantino, D. Daktarnieks, A. Duthie, A. Ienco, S. Midollini, C. Mitchell, A. Orlandini, L. Sorace, *Inorg. Chem.* **2005**, *44*, 9416–9423; b) S. Midollini, A. Orlandini, *J. Coord. Chem.* **2006**, *59*, 1433–1442; c) T. Bataille, F. Costantino, P. Lorenzo-Luis, S. Midollini, A. Orlandini, *Inorg. Chim. Acta* **2008**, *361*, 9–15; d) F. Costantino, A. Ienco, S. Midollini, A. Orlandini, L. Sorace, A. Vacca, *Eur. J. Inorg. Chem.* **2008**, 3046–3055.
- [35] a) T. Glowiak, W. Sawka-Dobrowolska, *Acta Crystallogr., Sect. B* **1977**, *33*, 2648; b) T. Glowiak, W. Sawka-Dobrowolska, *Acta Crystallogr., Sect. B* **1977**, *33*, 2763–2766; c) Z. Žák, J. Kožíšek, T. Glowiak, *Z. Anorg. Allg. Chem.* **1981**, *477*, 221–224; d) W. Sawka-Dobrowolska, T. Glowiak, *Acta Crystallogr., Sect. C* **1983**, *39*, 345–347; e) T. Glowiak, *Acta Crystallogr., Sect. C* **1986**, *42*, 62–64.
- [36] D. Fernández, D. Vega, A. Goeta, *Acta Crystallogr., Sect. C* **2002**, *58*, m494–m497; D. Fernández, D. Vega, A. Goeta, *Acta Crystallogr., Sect. C* **2003**, *59*, m543–m545.
- [37] E. Alvarez, A. G. Marquez, T. Devic, N. Steunou, C. Serre, C. Bonhomme, C. Gervais, I. Izquierdo-Barba, M. Vallet-Regi, D. Laurencin, F. Maurif, P. Horcajada, *CrystEngComm* **2013**, *15*, 9899–9905.
- [38] τ is a coefficient that reflects the shape of the coordination polyhedron: $\tau = 0$ for a tetragonal pyramid, and $\tau = 1$ for a trigonal bipyramid. See: A. W. Addison, T. N. Rao, J. Reedijk, J. van Rijn, G. C. Verschoor, *J. Chem. Soc., Dalton Trans.* **1984**, 1349–1356.

- [39] J. Notni, P. Hermann, J. Havlíčková, J. Kotek, V. Kubiček, J. Plutnar, N. Loktionova, P. J. Riss, F. Rösch, I. Lukeš, *Chem. Eur. J.* **2010**, *16*, 7174–7185.
- [40] V. Kubiček, P. Vojtíšek, J. Rudovský, P. Hermann, I. Lukeš, *Dalton Trans.* **2003**, 3927–3938.
- [41] C. F. Baes Jr., R. E. Mesmer, *The Hydrolysis of Cations*, Wiley, New York, **1976**.
- [42] M. Kývala, I. Lukeš, *International Conference, Chemometrics '95*, p. 63, Pardubice, Czech Republic, **1995**; the full version of the software *OPIUM* is available (free of charge) from: <http://www.natur.cuni.cz/~kyvala/opium.html>.
- [43] *SAINTE*, v. 8.32B, Bruker AXS Inc., Madison, USA, **2013**.
- [44] *SADABS*, v. 2012/1, Bruker AXS Inc., Madison, USA, **2012**.
- [45] G. M. Sheldrick, *SHELXS97 – A Computer Program for Solution of Crystal Structures*, University of Göttingen, Germany, **1997**.
- [46] G. M. Sheldrick, *SHELXL97 – Program for Crystal Structure Refinement from Diffraction Data*, University of Göttingen, Germany, **1997**.
- [47] A. L. Spek, *PLATON – A Multipurpose Crystallographic Tool*, Utrecht University, The Netherlands, **2011**; A. L. Spek, *Acta Crystallogr. D*, **2009**, *65*, 148–155.

Received: May 12, 2014
Published Online: July 30, 2014